Energy Storage for PV-Driven Air-Conditioning for an Off-Grid Resort – A Case Study

Christoph Luerssen[1,2], Arifeen Wahed[1], Thomas Reindl[1], Clayton Miller[2], David Cheong[2] and Chandra Sekhar[2]

[1] Solar Energy Research Institute of Singapore (SERIS), National University of Singapore (NUS), Singapore (Singapore)

[2] Department of Building, National University of Singapore (NUS), Singapore (Singapore)

Abstract

The current paper presents a case study of a PV-driven air-conditioning system with battery and latent heat storage applied for an off-grid resort in Bintan (Indonesia). The lead-acid battery bank has a nominal energy storage capacity of 47 kWh and the ice storage can store up to 92 kWh latent heat. The entire energy system of the resort was equipped with a comprehensive real-time data acquisition system to measure different parameters such as solar irradiation, temperatures, flow rates and power consumptions. More than 100 parameters are transferred minutely and monitored remotely across country borders. A TRNSYS model has also been developed to simulate the case study system dynamically. To assure accurate simulation results, the chiller and the Thermal Energy Storage (TES) models were calibrated using measured data from the monitoring system. Initial simulation results show the usage of the energy storages. The battery is utilised as a buffer to run the chillers with least disruptions and the TES is used to shift the cold generated during daytime to cool bedrooms at nighttime. The later one can also serve as a short-term energy storage over a few rainy days. For future works, we propose a comparative study of chilled water, ice and battery storage to design an optimal energy storage system for the resort based on the insights provided by this case study.

Keywords: Solar air-conditioning, PV-driven cooling, energy storage solutions, off-grid

1. Introduction

At present, a significant reduction in PV module costs pares the broader integration of PV systems. Hence, PV-driven cooling systems have gained attention. Compared to solar thermally driven cooling systems, at present PV-driven cooling systems' footprint is lower (Otanicar et al., 2012; Noro et al., 2014; Eicker et al., 2014) and they are economically more favorable (Otanicar et al., 2012; Noro et al., 2014; Eicker et al., 2014). The primary driver for the superior results of PV-driven cooling is the substantial decrease in PV costs and the higher Coefficient of Performance (COP) (Otanicar et al., 2012; Noro et al., 2014). Furthermore, the individual components are well-known, and the solution is flexible, which has the potential to improve situations in off-grid areas where grid-connections are not viable so far (Wang and Ge, 2016). However, there are challenges, since the PV power output does not match cooling demand, as the first depends on the solar irradiation whereas the second is also influenced by the ambient temperature and the occupancy. Thus, energy storage is required to buffer the imbalance between power demand and supply.

In the tropics, load-shifting is required to buffer energy and shift it from daytime to nighttime; occasionally also over a few rainy or cloudy days. Typically, battery storage technologies are considered for this energy storage duration of solar energy in an off-grid system (Merei et al., 2013; Eltawil, 2007). Looking at the Southeast Asian region in particular, a significant part of the energy consumption in buildings accounts for air-conditioning. This is a thermal load that allows for Thermal Energy Storage (TES). There are different TES solutions for cooling applications. Sensible energy storage is the most commonly realised in the form of chilled water (Arteconi et al., 2017). On district cooling scale or in large-scale office buildings also latent heat storage in the form of ice is common practice (Sehar et at., 2012; Chan et al. 20016). Other Phase Change Materials (PCM) have been commercialised and are investigated for application in TES systems (Souayfane et al., 2016; Ewert, 2000; Foster, 2017).

In grid-connected systems, the effective utilization of an energy storage such as a chilled water tank depends on the economic viability, i.e., increase the self-consumption of solar energy instead of selling it to the grid for a lower price

doi:10.18086/swc.2017.28.14 Available at http://proceedings.ises.org

(Arteconi et al., 2017). However, in an off-grid environment, energy storage is a necessity. An off-grid PV-driven cooling system can be configured as shown in Figure 1. Energy generated by a PV system is often stored directly via a battery. However, it is also possible to store the cold produced by the chiller via TES.

A prototype of such a system using latent heat and battery storage is installed at the LooLa resort in the rural and remote south-east of Bintan Island (Pulau Bintan) in the Riau Archipelago of Indonesia. The resort focusses on environmental and sustainable aspects as well as empowering their local staff and it is not connected to the public grid. The Solar Energy Research Institute of Singapore (SERIS) was selected as an R&D partner to monitor the existent prototype to optimise its performance and use it as a starting point for further investigation and research.

The objective of the present case study is to gain insights regarding operational and energy performance. It prepares a comparative study of different energy storage for the PV-driven cooling system at the resort. Therefore, the existing system is described, equipped with a monitoring system and dynamically modelled. Preliminary results are shown and research opportunities are discussed to round the study off.

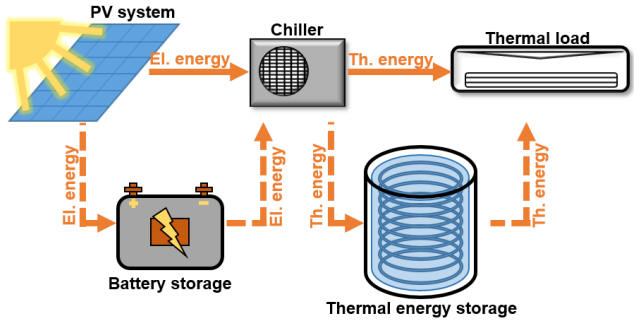

Fig. 1: Schematic of the system concept of an off-grid solar PV-driven air-conditioning system showing the variety of energy storage opportunities.

2. Case study description

The LooLa eco-resort has two villas offering higher-class hotel rooms with air-conditioning at night. To demonstrate sustainable technologies, a prototype of a PV-driven air-conditioning system was implemented in each of the villas. Additionally, a diesel generator is operated during nighttime to augment the power requirement in the resort. There is no public electricity grid access available in this part of Bintan. The main components of the PV powered air-conditioning system are electrical in nature including the PV system, the diesel generator and the chillers. It is only after the chillers that there is the switch to a thermal energy system as shown in Fig. 2.

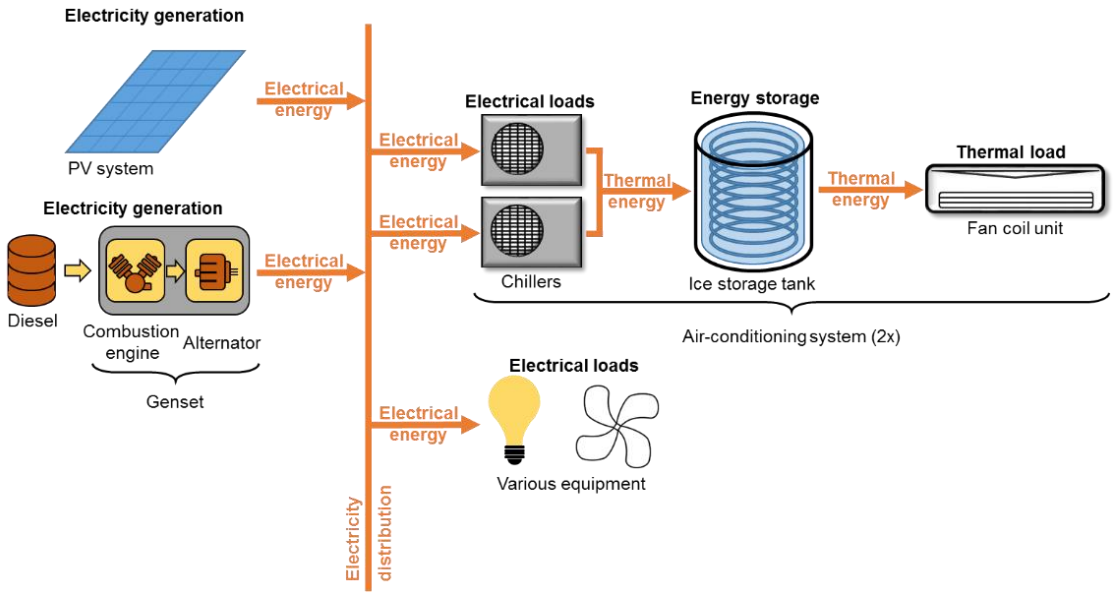

Fig. 2: Schematic of the energy system of the resort. On the left side PV system and diesel generator supply electricity to the distribution network. On the right side, both electrical and thermal loads are shown.

The PV system consists of different components – PV modules, PV inverters, batteries and battery inverters. During

daytime, it powers the air-conditioning systems for storing solar energy in the form of ice and supplies power for the shop, kitchen and office. The space cooling is scheduled to operate only during nighttime by discharging the thermal energy from the ice storage tank. To maintain the set point (room) temperature, FCUs supply cold air utilizing the latent energy from the ice storage tank without the need of operating the energy-intensive chillers. From 5.00PM to 8.00AM, the diesel generator supplies electricity for the entire resort. The switching of power sources is not automated, but manually conducted. An overview of the systems' and components' specifications is provided in Table 1.

Tab. 1: System and components specifications of the energy system at the LooLa resort

System	Component	Quantity	Specifications
PV system	PV module	72	Chinaland Solar Energy CHN240-60P; module power 240 W_p; multicrystalline silicon cells; 6 strings each having 12 modules; system power 17.3 kW_p
	Battery	48	RITAR OPzV2-490; tubular plate VRLA gel battery; capacity 490Ah
	PV inverter	3	SMA Sunny Boy 5000TL; rated AC power 4600 W
	Battery inverter	2	SMA Sunny Island 6.0H; rated AC power 4600 W; battery depth of discharge 50%
Diesel generator	Diesel Generator	1	Power 30 kVA
Two air-conditioning systems	Condensing unit	4 (2 per system)	Tecumseh FHT4525YHR; cooling capacity 2.4 kW and Power consumption 1.5 kW at 32 °C ambient temperature and -15 °C evaporation temperature; refrigerant R134a
	Evaporator (Heat exchanger)	4 (2 per system)	Gimleo GBH05-CMF; tube in shell heat exchanger; cooling capacity 9.5 kW
	Ice storage tank	2 (1 per system)	Customized design (cuboid shape); volume 1045 l; fiberglass; copper pipe; 15 cm Polyurethane foam insulation
	Water tank	2 (1 per system)	Guangdong LuckingStar New Energy LWT300-T&H-02; volume 300 l; stainless steel
	Fan coil unit small	6 (3 per system)	Eurostars 300WM2; cooling capacity 2.9 kW (max); power consumption 52 W
	Fan coil unit big	2 (1 per system)	Eurostars 400WM2; cooling capacity 3.7 kW (max); power consumption 62 W

2.1. Air-conditioning system design and operation

In order to understand the air-conditioning system design and operation, we look at a single air-conditioning system. The top part of Fig. 3 shows a simplified schematic focusing on the heat exchangers and fluid circuits. This schematic includes only one chiller, whereas the real system has two chillers. Therefore, the bottom part of Fig.3 provides a complementary Piping & Instrumentation (P&I) diagram for deeper understanding of the actual design. The top and the bottom part of Fig. 3 are linked in terms of color coding of key components.

At daytime, the chillers (conventional vapor-compression systems consisting of compressor, condenser, evaporator, expansion valve and refrigerant) operate at an evaporation temperature of below 0 °C. The chiller refrigerant exchanges heat to the ethylene glycol based water solution (glycol) in the evaporator. The glycol flows through the left side of the circuit in order to exchange heat with the water in the ice storage tank. The process is carried out through a tube and shell heat exchanger. Since the temperature of the glycol is below 0 °C, ice is generated in the storage tank. The ice storage is charged and the thermal energy is stored as latent heat.

During nighttime, the glycol exchanges heat with the ice in order to cool the water in the water tank to ~17 °C temperature. The chilled water from the water tank is pumped through the fan coil units that blow the cool air out, providing thermal comfort in the sleeping areas. The air-conditioning operation causes melting of the ice, i.e., discharging of the thermal energy storage.

On a sunny day, the condenser units and the auxiliary equipment run on the PV system for 8 hours, from 8AM to 4PM. In case of heavy rains and prolonged presence of clouds, the PV system is disconnected manually at the discretion of the operators, which means that there is no electricity available in the resort at that time. The loads are then manually reconnected to the PV system when the weather changes to more favorable conditions. This procedure is conducted to keep some buffer storage in the batteries. If there is not enough cooling energy stored in the thermal energy storage on a cloudy or rainy day, the chillers are powered by the batteries of the PV system until they are completely discharged. At night, the auxiliary power for devices such as pumps, valves and FCUs are sourced from the diesel generator.

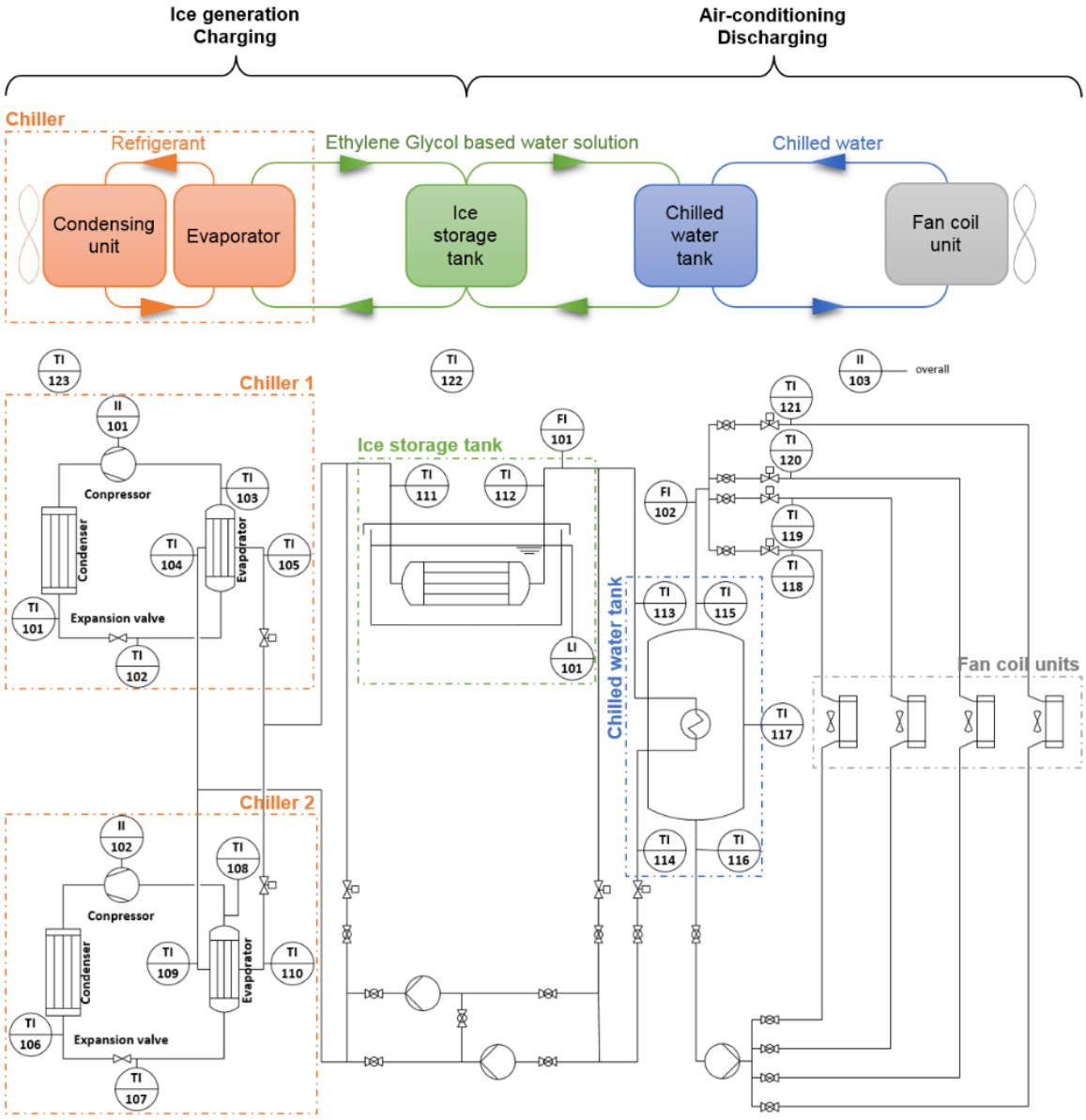

Fig. 3: Simplified schematic diagram describes the operation process of an air-conditioning system with thermal energy storage (top); Piping and Instrumentation diagram of a single air-conditioning system to show the sensor positions: temperature indicator (TI), flow indicator (FI), level indicator (LI), power indicator (II) (bottom)

3. Monitoring system

The prototypes of the PV-driven cooling systems enable the LooLa resort to provide air-conditioning to the clients

staying in the villas in an ecological way. However, the assessment of the performance was not possible due to insufficient data acquisition. Therefore, deployment of a monitoring system was the consequence. The developed monitoring architecture acquires sensor data throughout the entire resort. Three remote stations were deployed, one for each air-conditioning system and one that acquires PV system and diesel generator data. The top part of Fig. 4 shows the monitoring system architecture. On the field level, the relevant heat flows, components' performances/statuses and power consumptions need to be identified. Therefore, the ultrasonic flowmeters, ultrasonic level sensors for the ice storage tanks, temperature sensors and a silicon irradiance sensor are required for the PV and the cooling system. The sensors are hardwired to National Instruments (NI) CompactRIO controllers (cRIO), which are part of the control level. The remote stations consist of a cRIO, an Ethernet switch and a router. The bottom part of Fig. 4 provides a photo of one remote station and its components. They are lightning protected and backed-up through an uninterruptible power supply. The three cRIOs are capable of processing the acquired parameters remotely and fully automated. The LabVIEW software is capable to acquire the data from all the sensors as well as power meters and inverters. The later ones are directly accessed by MODBUS TCP. The cRIOs log the acquired data and transfer it from the remote stations in Bintan to the Central Monitoring Station (CMS) in Singapore by use of cellular network routers. The cellular network was observed to be rather weak at the resort and its vicinity. In order to find the most suitable locations for the routers, location-based tests were conducted a priori. Three spots, all close to one of the cRIOs, were found to have sufficient coverage for the data transmission. The routers are configured for a local SIM card and Virtual Private Network (VPN) to access the internet. At the process control level, the CMS receives one-minute live-data and initiates nightly download routines. The data is sorted into files and databases by the CMS to make it available for analysis.

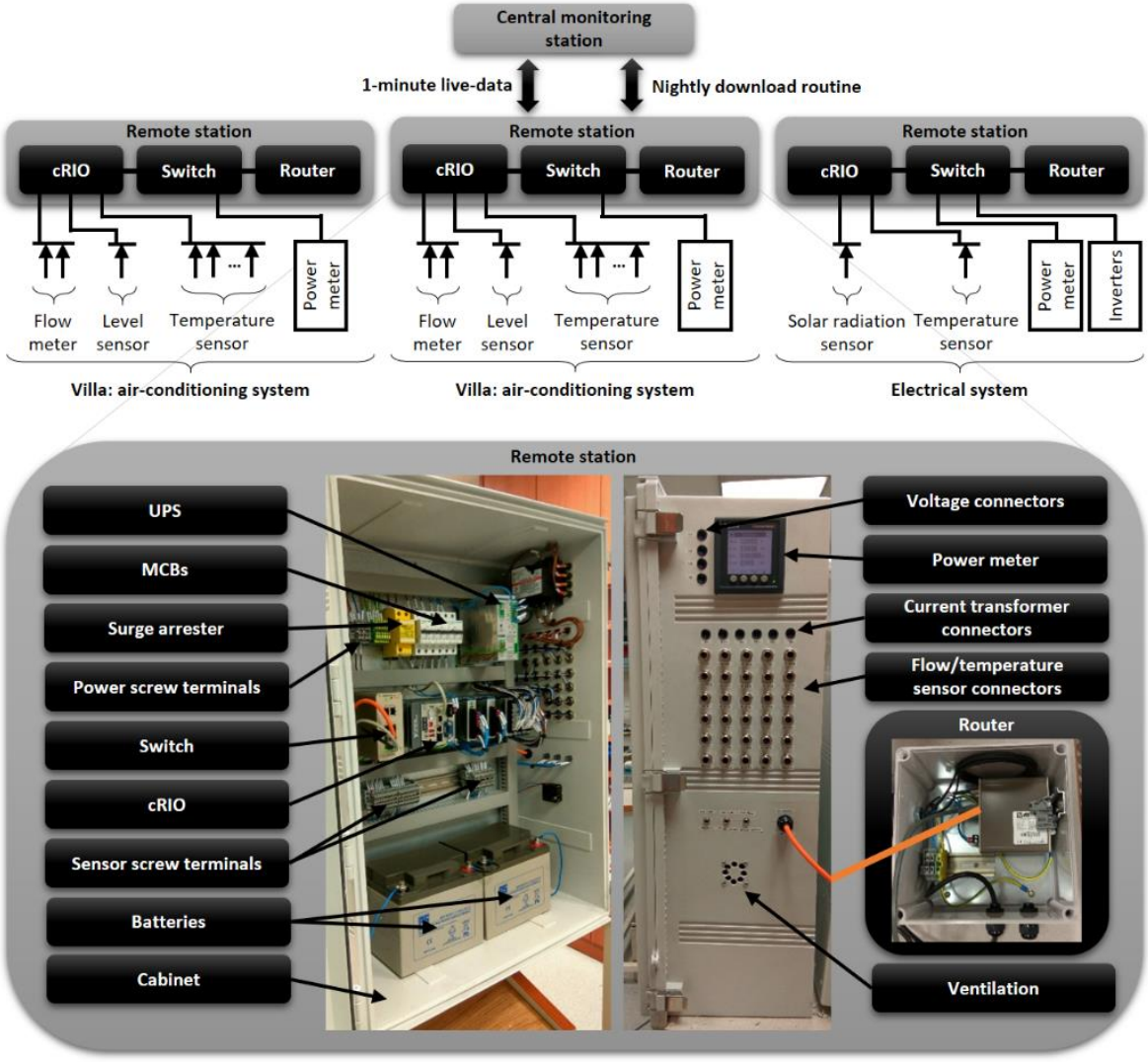

Fig. 4: System architecture of the monitoring system for the energy system at the LooLa resort (top); exemplary remote monitoring station (bottom)

This case study uses data measured by temperature sensors, flow meter and power meter to calibrate parts of a simulation model in Chapter 5. Detailed specifications of the utilised sensors is given in Table 2. To ensure the accuracy of the sensor/meter readings, additional calibration of certain sensors is required. The manufacturer of the temperature sensors provides accuracy class A. However, an additional multi-point calibration with a reference sensor (Isotech Hyperion Site & 935-14-61, overall accuracy: 0.04 °C) was conducted in a cooling bath from -20 °C to 40 °C for each sensor under laboratory conditions. The ultrasonic flow meters are also calibrated for the respective pipe dimensions and fluids, following similar laboratory conditions on-site. The calibration was conducted for the range of 0 to 15 l/min with an in-line reference flow meter (Rosemount 8732E, overall accuracy: ±0.02349 l/min). For both temperature sensors and flow meters, regression analysis was implemented in order to determine the correlation factors. The power meter meets IEC 61557-12 requirements and needs no further calibration.

The sensors were installed according to the P&I diagram in the bottom part of Fig. 3. Condensation and evaporation temperatures of the vapor-compression cycles are measured as well as stream temperatures before and after the ice storage tank, water tank and FCUs. Additionally, the water tank is equipped with a sensor measuring the temperature inside. The flow rates of the glycol and water are measured to be able to calculate the transferred thermal energy. The power meter measures the power consumption of the two chillers and the overall air-conditioning system.

Tab. 2: Specifications of the utilized sensors of the monitoring system

Parameter	Sensor	Range	Accuracy
Temperature	RTD, PT100, 4-wire, Thermotron	-30 to 100 °C	Class A
Flow rate	Ultrasonic flow meter Transmitter: Flexim F704 Transducer: Flexim FSQ	Plow velocity 0.01 to 25 m/s	Repeatability 0.15 % of reading ±0.01 m/s With standard calibration ±1.6% of reading ±0.01 m/s
Power	Current and voltage Schneider Electric PM5320	Depends on current transformers	Class 0.5S

4. Simulation model

A simulation model for the PV-driven cooling system at LooLa was set up using TRRNSYS 17.1, a dynamic simulation software. The model is divided into three main parts, cooling system 1, cooling system 2 and PV system, as displayed in Fig. 5. Additionally, weather data is utilised by all three parts. In the bottom part of Fig. 5, the outputs are processed, plotted and compiled in a text file for further analysis.

Cooling system 1 represents the actual system described in Chapter 2.1. Two chillers charge the ice storage tank (provided by Lerch and Heinz (2012)) during scheduled hours at daytime. Similar to the real system, the air-conditioning is scheduled during certain hours at night. Additionally, an occupancy calendar using the booking data of the resort in 2016 was implemented. The given data provides information about whether a villa is booked, but not how many rooms in which villa are booked, hence the occupancy is a binary input. In the discharging circuit, the chilled water tank was replaced by a controlled tempering valve keeping the glycol solution temperature at 12 °C and the four FCUs are simulated using a single FCU model. The input parameters for the FCU were determined using the psychrometric chart in Fig. 6. The return air is mixed with 15% outdoor air. One air change per hour is achieved by an air flow rate of 790 kg/h for four bed areas, each 12.5 m² and 2 m celling height. This results into a cooling load of 2.76 kW according to the mixed air and supply air conditions from the psychometric chart.

Cooling system 2 is only represented by the electrical load of the two chillers, because the system is similar to cooling system 1. The PV system powers the four chillers of the cooling systems. The power consumption of the auxiliary equipment, such as pumps, valves, control and FCUs, as well as the other loads at the resort that are connected to the PV system are neglected. The parameters for PV modules, batteries and control strategy are chosen according to the on-site system.

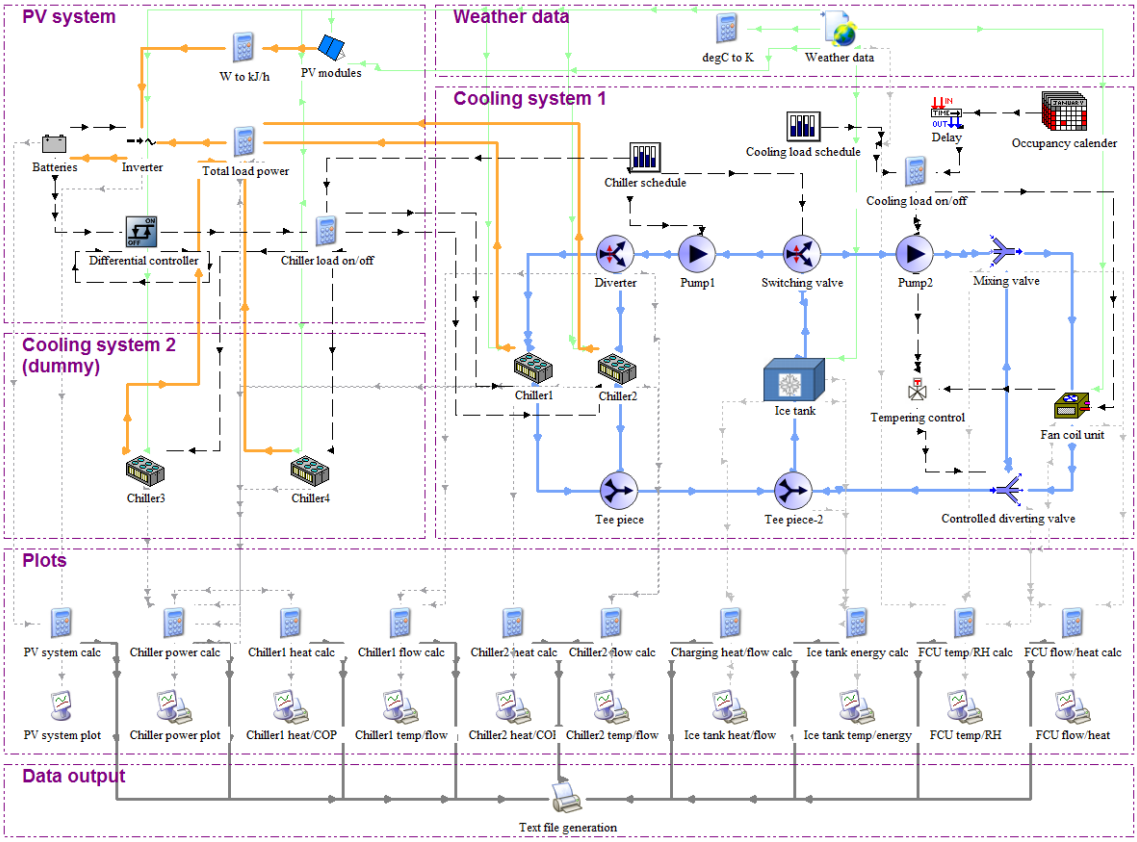

Fig. 5: TRNSYS simulation model of the PV-driven cooling system at the LooLa resort; Lines: power line – orange bold, weather data – green, output data – grey dotted, control lines – black dashed, pipes – blue bold.

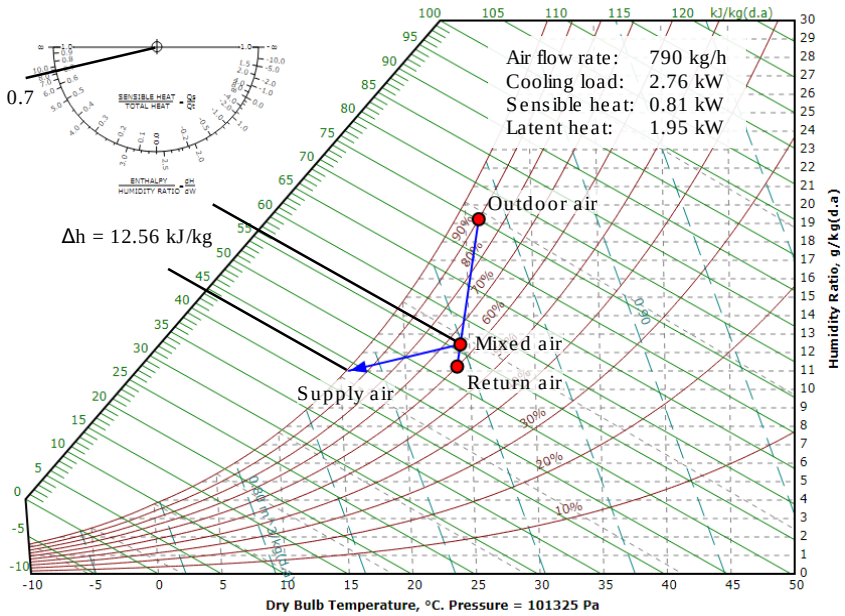

Fig. 6: Cooling load estimation via psychrometric chart; created with http://www.flycarpet.net/en/PsyOnline

5. Calibration results

The critical components, chiller and TES, were tested utilising data acquired by the monitoring system. Therefore, a simplified version of the simulation model was used, see Fig. 7. The chiller model is from the TESS library, Type655 and cuboid storage tank model Type843 was developed by Lerch and Heinz (2012). The TES model can operate as chilled water and ice tank.

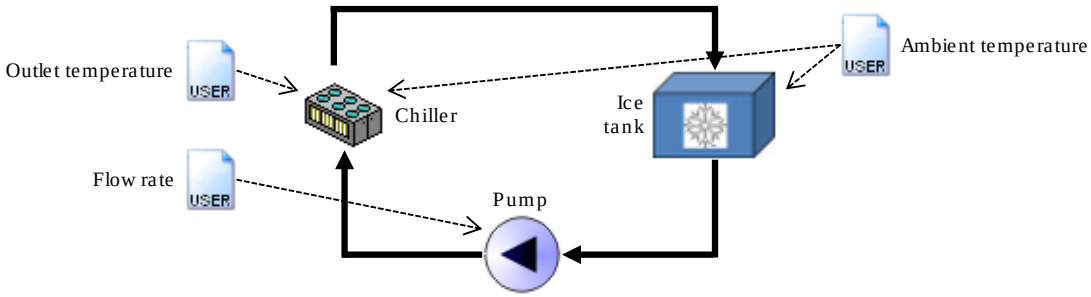

Fig. 7: Simplified TRNSYS simulation model for calibration of chiller and storage tank with measured data inputs

First, the operation as chilled water tank during charging is tested. Therefore, eight hours of measured data with the sample rate 1/min for chiller outlet temperature, ambient temperature and flow rate are used as inputs for the model. The model outputs to be compared with actual measured data are chiller power and tank outlet temperature. The result is plotted in graph 1a and 2a in Fig. 8. The non-fitting chiller power graph is caused by the performance data files of Type 655 that assume the chiller to be capable of operating in part load, which is not the case in the actual system. After adjustment of the performance data files, the Root Mean Square Error (RMSE) is merely 30 W as shown in graph 1b (Fig. 8). The tank outlet temperature decreases faster in the simulation than in the real setup, when the tank inlet temperature is prescript by measured data. This means that the actual heat transfer is lower than the simulated heat transfer. As the heat depends on flow rate, temperature difference and specific heat, where the temperature difference and the flow rate are measured, the specific heat serves as a parameter to match the model performance with the actual performance; the value is adjusted from 3.54 kJ/kgK to 1.7 kJ/kgK. The result is plotted in graph 2b of Fig. 8 and the RMSE has decreased to 0.18 °C.

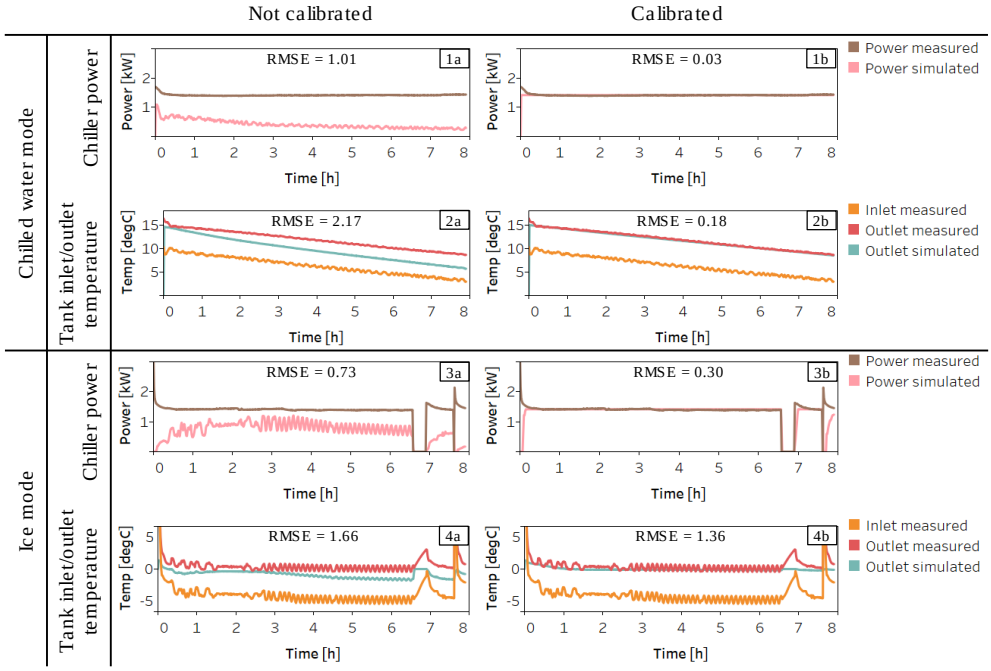

Fig. 8: Calibration of the chiller and storage tank models in chilled water mode (top) and ice mode (bottom) with measured data

The calibrated model represents the actual system accurately as shown by the RMSE values. However, the TES from Lerch and Heinz (2012) can also simulate the phase change from water to ice and, hence, operate as latent heat storage. Therefore, the input data from a day where the TES operates as ice tank during charging is chosen to test the simulation model for this condition. The simulation was run without calibration (graphs 3a and 4a in Fig. 8) and with the calibration measures described above (3b and 4b in Fig. 8). The chiller power RMSE is ten times higher compared to the chilled water operation, however a precise fit can be observed between 0.5 h and 6.5 h. in graph 3b (Fig. 8). The increased error is caused by two operation interruptions after 6.5 h and the starting current that is not modeled. The increase of the RMSE for the outlet temperature can be explained by the chiller operation interruptions as well. An additional factor is the oscillating temperature sensor reading that might have been caused by parasitic frequencies along the sensor wires. Overall, the TRNSYS simulation models the real system sufficiently accurate to produce

initial annual simulation results.

6. Initial simulation results

The TRNSYS simulation was performed for an entire year (8760 h) with a time step of 0.5 h. The initial results discussed in this chapter focus on the utilisation of the energy battery storage (Fig. 9) and the TES (Fig. 10).

The battery is charged to store surplus solar energy and discharged to supply energy for the chillers in case of insufficient solar energy availability. The usable storage capacity is 23.5 kWh considering 50% DoD. The four chillers consume 5.67 kW, which means the battery will ensure continuation of chiller operation for 4.15 h when it is fully charged. On a rainy or overcast day, chiller operation disruptions can occur due to the battery being fully discharged. This situation can be seen in the bottom chart of Fig. 9 when the graph approaches 0 kWh stored energy. Furthermore, the chart shows a high cycling frequency, which means that the battery serves as buffer storage. The bar chart in the top of Fig. 9 supports the finding, as the daily charged and discharged energy even exceeds the usable storage capacity of the battery (23.5 kWh) on many days. On those days, more than one cycle is performed.

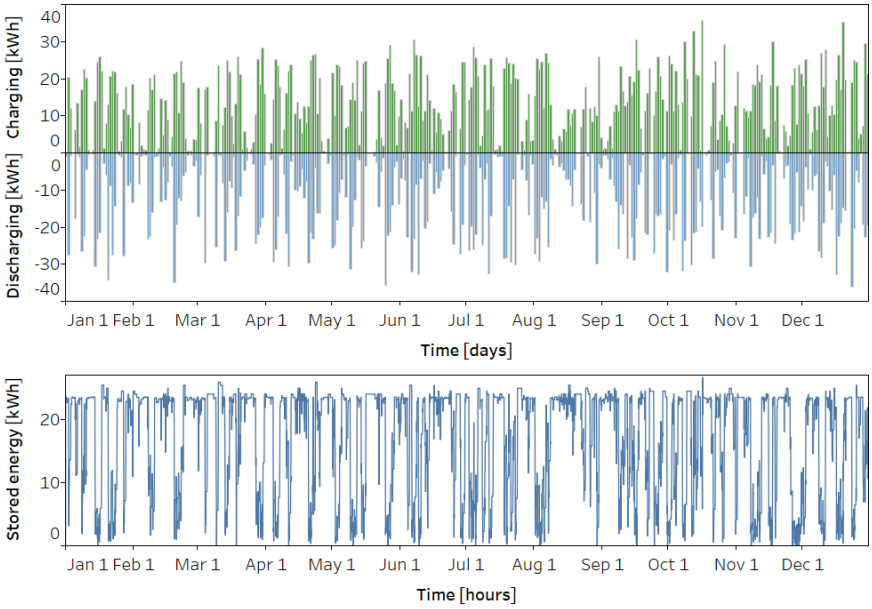

Fig. 9: Battery storage utilization; daily charged and discharged energy (top); stored energy again hours (bottom)

While the utilization of the battery storage occurs during chiller operation hours at daytime, the TES is only charged during that time. The discharging happens at nighttime. Unlike the battery, charging and discharging of the TES cannot occur simultaneously. Thus, the bottom graph of Fig. 10 (stored energy in the TES against time) shows a different pattern than the bottom graph of Fig. 9 (stored energy in the battery against time). The TES is charged nearly every day, but the discharging depends on the occupancy calendar; no occupancy means no discharging (see top chart in Fig. 10). The amount of charged energy (top chart in Fig. 10) decreases with increasing amount of energy stored, because the ice generated in the tank has lower heat conductivity than water, hence, insulating properties. Furthermore, the daily amount of charged energy also depends on the chiller operation hours during that day. In Fig. 10, 0 kWh stored energy is defined as 0% ice in the tank. Below that, it operates as chilled water tank. During high occupancy in December, the tank operates frequently as chilled water tank and might not meet the space cooling requirements.

The TES is cycled less frequently compared to the battery storage. It can store up to 93 kWh of latent heat, approximately four times the storage capacity of the battery. Thus, the TES serves as short-term energy storage that can shift the energy generated during daytime to serve the cooling needs during nighttime. Moreover, it can supply sufficient cooling over a few rainy or cloudy days.

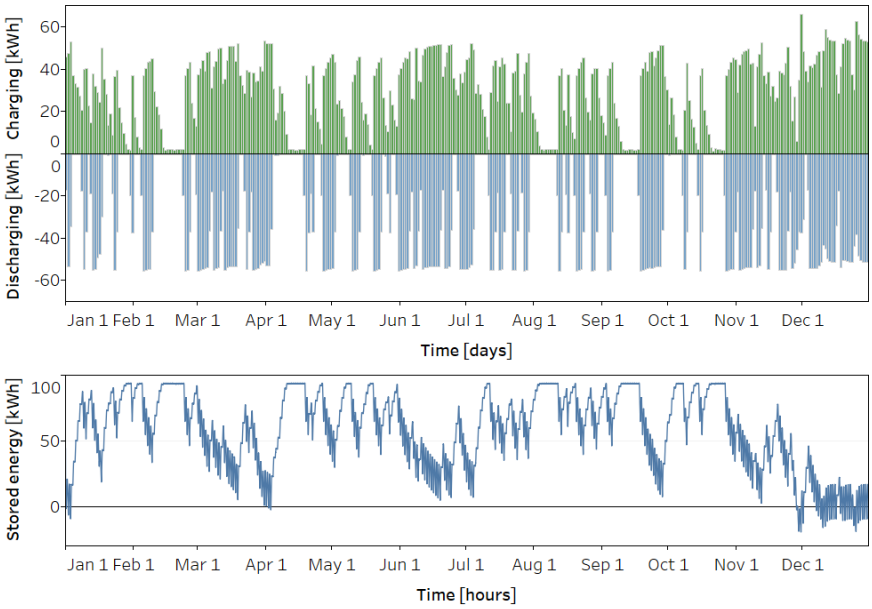

Fig. 10: TES utilization; daily charged and discharged energy (top); stored energy again hours (bottom)

7. Conclusion and outlook

The case study system is monitored in real-time and the data is used to calibrated components of a simulation model. Initial results emphasise the role of the battery and TES in the operation of this PV-driven cooling system. However, the simulation reflects not exactly the on-site situation, because of the following simplifications:

- The load of the PV system consists only of the chiller power consumption. In reality other parts of the resort (e.g. kitchen, shop and office) are also powered by the PV system during daytime, hence frequency of the power outages is likely to be higher.
- The power consumption of the auxiliary equipment of the cooling system, e.g. pumps, valves and control, were neglected. They are powered by the PV system during daytime and by the diesel generator during nighttime.
- The TRNSYS chiller model Type 655 requires a set temperature input, but the real chillers do not have a set temperature; only the evaporation temperature can be adjusted through the expansion valve.
- The cooling load was estimated via space volume and psychrometric chart and not derived from measured data. Furthermore, a binary value was used for the occupancy due to limited booking data.
- On the thermal load side, the water tank and 4 FCUs were replaced by a single FCU and a tempering valve.
- The charging process of the TES was only calibrated by a data set of 8 h and the discharging process was not calibrated.
- Pipe losses were not considered in this simulation.

Further work on enhance the simulation model will be done. Subsequently, three main topics will be addressed to complete the case study:

- A parametric study to size a battery storage, a chilled water tank and an ice storage tank for the prototype system.
- An economic analysis of the PV-driven cooling system at the LooLa resort.
- A comprehensive comparative study of the PV-driven cooling system with the three different energy storage solutions compared to a baseline system powered by a diesel generator in terms of energy and economic performance.

Eventually, the modelling and analysis shall be generalised towards a workflow that can be applied to various cooling applications.

8. Acknowledgements

The study is part of a research project funded by the LooLa Adventure Resort. The authors gratefully acknowledge the cooperation with the local LooLa staff in Bintan and the CEO, Dr. Marc van Loo. Moreover, we want to thank Shantanu Vachhani, a SERIS intern, for investigating various TES models and selecting the ice tank model for this paper. We are glad to be able to fall back on his work, when selecting the ice tank model for this paper. Last but not least, we are more than grateful for the selflessness of Dr. Andreas Heinz who provided the utilised ice tank model (Type 843) for this study.

9. References

Arteconi, A., Ciarrocchi, E., Pan, Q., Carducci, F., Comodi, G., Polonara, F., Wang, R., 2017. Thermal energy storage coupled with PV panels for demand side management of industrial building cooling loads. Applied Energy 185, 1984–1993.

Chan, A.L.S., Chow, T.-T., Fong, S.K.F., Lin, J.Z., 2006. Performance evaluation of district cooling plant with ice storage, Energy 31, 2750–2762.

Eicker, U., Colmenar-Santos, A., Teran, L., Cotrado, M., 2014. Economic evaluation of solar thermal and photovoltaic cooling systems through simulation in different climate conditions: An analysis in three different cities in Europe. Energy and Buildings 70, 207-223.

Eltawil, M.A., Samuel, D.V.K., 2007. Vapour Compression Cooling System Powered By Solar PV Array for Potato Storage. Agricultural Engineering International: the CIGR Ejournal. Manuscript EE 06003. Vol. IX.

Foster, R., Jensen, B., Dugdill, B., Hadley, W., Knight, B., Faraj, A., Mwove, J.K., 2017. Direct Drive Photovoltaic Milk Chilling Experience in Kenya. IEEE Photovoltaic Specialists Conference 44.

Ewert, M.K., Bergeron, D.J., Foster, R.E., LaFleur, 2002. Photovoltiac direct-drive, battery-free solar refrigerator field test results. Solar 2002 - American Solar Energy Society.

Lerch, W., Heinz, A., 2012. Solare Wärmepumpen – Kombianlagen inkl. Abwasser Wärmerückgewinnung: Energetische Bewertung durch dynamische Anlagensimulationen in TRNSYS, Solar 2012, Gleisdorf (Austria).

Merei, G., Berger, C., Sauer, D.U., 2013. Optimization of an off-grid hybrid PV–Wind–Diesel system with different battery technologies using genetic algorithm. Solar Energy 97, 460–473.

Noro, M., Lazzarin, R.M., 2014. Solar cooling between thermal and photovoltaic: An energy and comparative study in the Mediterranean conditions. Energy 73, 453-464.

Otanicar, T., Taylor, R.A., Phelan, P.E., 2012. Prospects for solar cooling – An economic and environmental assessment. Solar Energy 86, 1287-1299.

Sehar, F., Rahman, S., Pipattanasomporn, M., 2012. Impacts of ice storage on electrical energy consumptions in office buildings, Energy and Buildings 51, 255–262.

Souayfane F., Fardoun, F., Biwole, P., 2016. Phase change materials (PCM) for cooling applications in buildings: A review. Energy and Buildings 129, 396–431.

Wang, R.Z., Ge, T.S., 2016. Advances in Solar Heating and Cooling, Elsevier, United Kingdom.